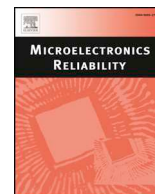




ELSEVIER

Contents lists available at ScienceDirect

Microelectronics Reliability

journal homepage: www.elsevier.com/locate/microrel

Power switch failures tolerance of a photovoltaic fed three-level boost DC-DC converter

Driss Oulad-Abbou^{a,b,*}, Said Doubabi^a, Ahmed Rachid^b

^aLaboratory of Electric Systems and Telecommunications, Cadi-Ayyad University, BP 549, Av Abdelkarim Elkhatabi, Gueliz, Marrakesh, Morocco

^bLaboratory of Innovative Technologies, University of Picardie Jules Verne, Amiens, France

ARTICLE INFO

Keywords:

DC-DC converters
Three-level boost DC-DC converter
Fault tolerant
Fault detection and diagnosis

ABSTRACT

In this paper, both switches open/short circuit faults diagnosis and a fault tolerant diagram of a photovoltaic (PV) fed Three-Level Boost DC-DC Converter (TLBDC) are addressed. Diodes voltages are used to detect open or short circuit faults. These voltages are also used to ensure voltage balance control of the TLBDC. Hence, the number of sensors would be the same as the number of sensors used in a conventional TLBDC controller scheme. The proposed method identifies and locates the faulty switch easily. The TLBDC is reconfigured where the ensured input power and output voltage remain unchanged. This is achieved by adding only one extra power switch to the TLBDC topology. Simulation and experimental results confirm the effectiveness of the proposed fault diagnosis method and the TLBDC fault tolerant scheme.

1. Introduction

Around the world, renewable energy use is under rise. This alternative energy source holds the key to combating climate change. The most common sources are: solar, wind, hydro, geothermal and biomass. Solar Photovoltaic (PV) is one of the promising sustainable energy sources. PV modules are composed of semiconductors that allow the direct transformation of sunlight into electricity. These modules require very little maintenance and the majority of manufacturers offer long period warranties. Millions of PV systems have been installed in the whole world, with different power levels, ranging from a fraction of a watt to several megawatts. For several applications, PV systems are not only cost-effective, but they can also be the least expensive option.

PV systems can be classified into three types: standalone, grid connected and hybrid systems. These PV systems use Maximum Power Point tracking (MPPT) controlled DC-DC converters to interface the PV source to the loads [1–10]. These converters play a main role in PV systems, since they directly connect the PV source to the load. DC-DC converters are mainly composed of power switches, where failures occurrence may involve an interruption of power extraction from the PV source and hence leads to significant energy losses.

Electrical and thermal stresses excess is the main cause of power switches failures [11]. These failures can be classified as open and short circuit faults. To avoid such undesirable scenarios, fault tolerant DC-DC

converters should be developed. Various power switch fault-diagnosis methods and fault-tolerant strategies were applied to rectifiers and to several inverters topologies [12–17].

DC-DC converters have benefited from fault tolerant strategies [11], [18–26]. Fault tolerant operation of modular multilevel converters using redundant modules were introduced in [25,26]. In [26] the authors proposed a fault tolerant input parallel output series DC/DC converter. Redundant modules were employed to allow circuit re-configuration by bypassing faulty modules using a combination of bypass switches and bleed resistors. In [27], parallel and series connected backup switches and diodes were used to allow faulty operation of a 5-level generalized multilevel converter. However, additional current sensors are required to locate faults, which increases the cost and system complexity. In [28], the variation in power switch ON resistance was used to detect the switches failures of basic DC-DC converters. This resistance was calculated using the inductor current frequency response. The authors in [29] have discussed and analyzed the operation under different faults of a conventional DC-DC Boost converter. This facilitates the fault tolerant converter design and implementation. Monitoring and diagnosis of DC-DC converters using the near magnetic field have been presented in [20]. However, a near field probe is required to capture the magnetic field, which increases the cost and system complexity.

In [24], a Three-Level Boost DC-DC Converter (TLBDC) of a PV

* Corresponding author at: Laboratory of Electric Systems and Telecommunications, Cadi-Ayyad University, BP 549, Av Abdelkarim Elkhatabi, Gueliz, Marrakesh, Morocco.

E-mail addresses: driss.oulad-abbou@etud.u-picardie.fr (D. Oulad-Abbou), s.doubabi@uca.ac.ma (S. Doubabi), ahmed.rachid@u-picardie.fr (A. Rachid).

<https://doi.org/10.1016/j.microrel.2018.11.017>

Received 7 August 2018; Received in revised form 20 November 2018; Accepted 26 November 2018

Available online 30 November 2018

0026-2714/ © 2018 Elsevier Ltd. All rights reserved.

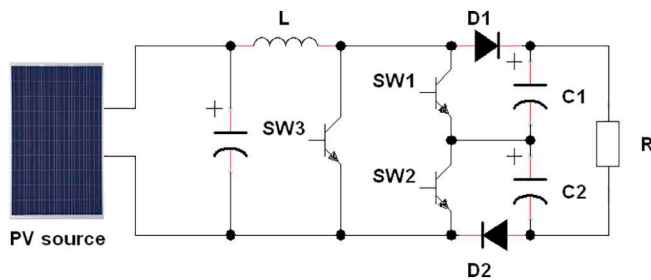


Fig. 1. The proposed TLBDC fault tolerant scheme.

based fault tolerant converter was proposed. The unbalance of TLBDC output capacitors' voltages was used to detect and locate the switches open circuit faults. Four additional switches were placed in parallel to the TLBDC switches and capacitors to permit faulty operation, where the converter operates as a conventional boost DC-DC converter.

A fault-tolerant strategy for a PV fed TLBDC was presented in [11]. The TLBDC is supplied by two series connected PV modules. The fault occurrence is detected when a suddenly input current drop and input voltage increase are observed. Capacitors voltages unbalance was used to detect and locate the fault, and then reconfigure the circuit. In normal state, the converter operates as a TLBDC, PV voltage and current are the MPPT controller inputs. Output dc-link capacitors voltages are sensed and balanced via a PI Voltage Balance (VB) controller. After open circuit fault detection the faulty switch stops working and the TLBDC is reconfigured as a conventional two-level boost converter. The MPPT control is kept for only one PV module while the other one is operating without MPPT control. However, capacitors voltages balance is lost and the converter is providing less power than the one supplied in post fault.

Unlike the previous works that were focused only on switches open circuit faults diagnosis [11,18,24,30], this work is focused on TLBDC switches open and short-circuit faults diagnosis. The proposed TLBDC fault tolerant converter scheme is shown in Fig. 1.

The Fault detection is accurately ensured by the diodes' D1 and D2 average voltages. If one of these diodes average voltages is equals to the diode forward voltage drop, which means that the corresponding diode is forward biased continuously, a power switch fault (short or open circuit fault) is detected. The faulty switch (SW1 or SW2) is easily identified as the one nearby the continuously forward biased diode.

In addition, these diodes average voltages are also used for output capacitors VB control. Hence, no extra voltage sensors will be needed for VB control as shown in the controller schema depicted in Fig. 6. Therefore, the number of sensors used either for normal operation of a PV fed TLBDC and for the proposed fault tolerant TLBDC is the same.

During normal operation, the proposed fault tolerant converter operates as a TLBDC. The SW3 switch is uncontrolled while switches SW1 and SW2 are controlled using PWM signals phase-shifted by 180° (as shown in Fig. 2). In faulty mode, the converter operates as a conventional two-level boost DC-DC converter. SW3 is PWM controlled while SW1 and SW2 are uncontrolled.

In order to evaluate the effectiveness of the proposed fault tolerant strategy, two case studies were considered under simulation and on an experimental setup. The first test is related to an open circuit fault while the second one is related to short circuit fault. The sequence used in both tests is the following: at first the TLBDC operates without VB control, then the VB control is activated, followed by a fault occurrence (either open or short circuit fault). The simulation and experimental results illustrate the effectiveness of the proposed methodology.

The rest of the paper is organized as follows. Section 2 describes the proposed fault tolerant TLBDC operation. The Fault diagnosis and re-configuration method is presented in Section 3. The proposed fault tolerant TLBDC controller design is presented in Section 4. Finally

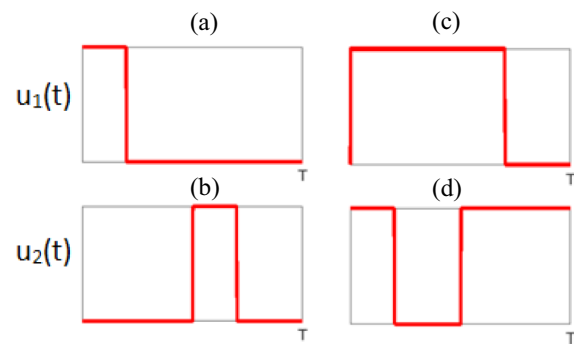


Fig. 2. Control signals of: (a) switch SW1 and (b) switch SW2 when the duty cycle is lower than 50%; (c) switch SW1 and (d) switch SW2 when the duty cycle is higher than 50%.

Table 1
Equivalent TLBDC circuit and diodes voltages for each operating state.

ST1	ST2	Equivalent circuit	Diode D1 voltage	Diode D2 voltage
0	0		V_f	V_f
1	0		$-VC1$	V_f
0	1		V_f	$-VC2$
1	1		$-VC1$	$-VC2$

results and discussions are presented in Section 5 followed by the conclusion.

2. Proposed fault tolerant three-level boost DC-DC converter operating principles

The electrical scheme of the proposed fault tolerant TLBDC is shown in Fig. 1. It is composed of an inductor L, three power switches SW1, SW2 and SW3, two switching diodes D1 and D2, and two electrolytic capacitors C1 and C2.

During normal operation, the converter operates as a TLBDC, where the switches SW1 and SW2 control signals are PWM signals phase-shifted by 180°, as illustrated in Fig. 2, while switch SW3 control signals is set to zero.

Based on the control signals illustrated in Fig. 2, four operating cases could be distinguished. For each case, the converter is described by an equivalent electrical scheme and equations, these schemes are summarized in Table 1 and the detailed description of the equations that describe the converter operation is presented in [31]. ST1 and ST2 are switches SW1 and SW2 states, respectively. If ST1 (ST2) is equals to 1, then SW1 (SW2) is ON and if ST1 (ST2) is null, this means that SW1

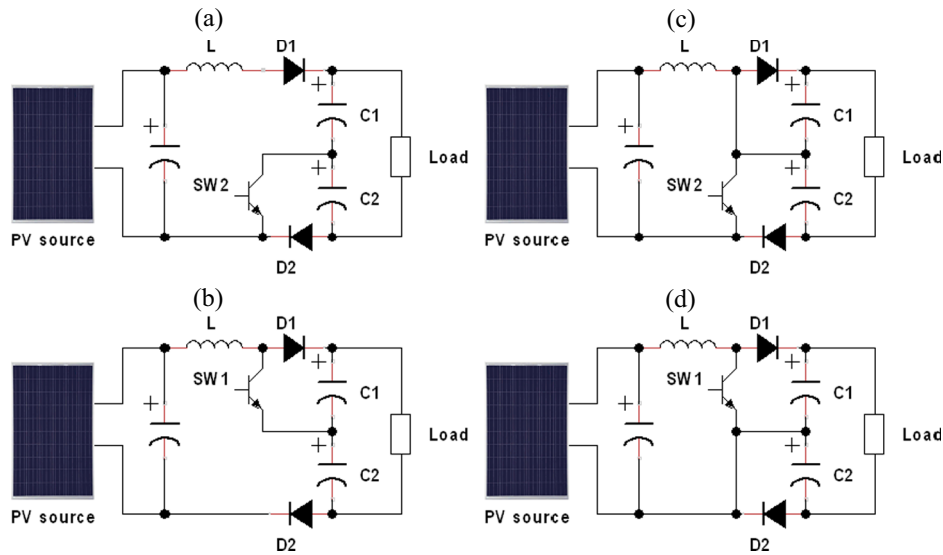


Fig. 3. TLBDC considered faulty cases: (a) SW1 open circuit fault, (b) SW2 open circuit fault, (c) SW1 short circuit fault and (d) SW2 short circuit fault.

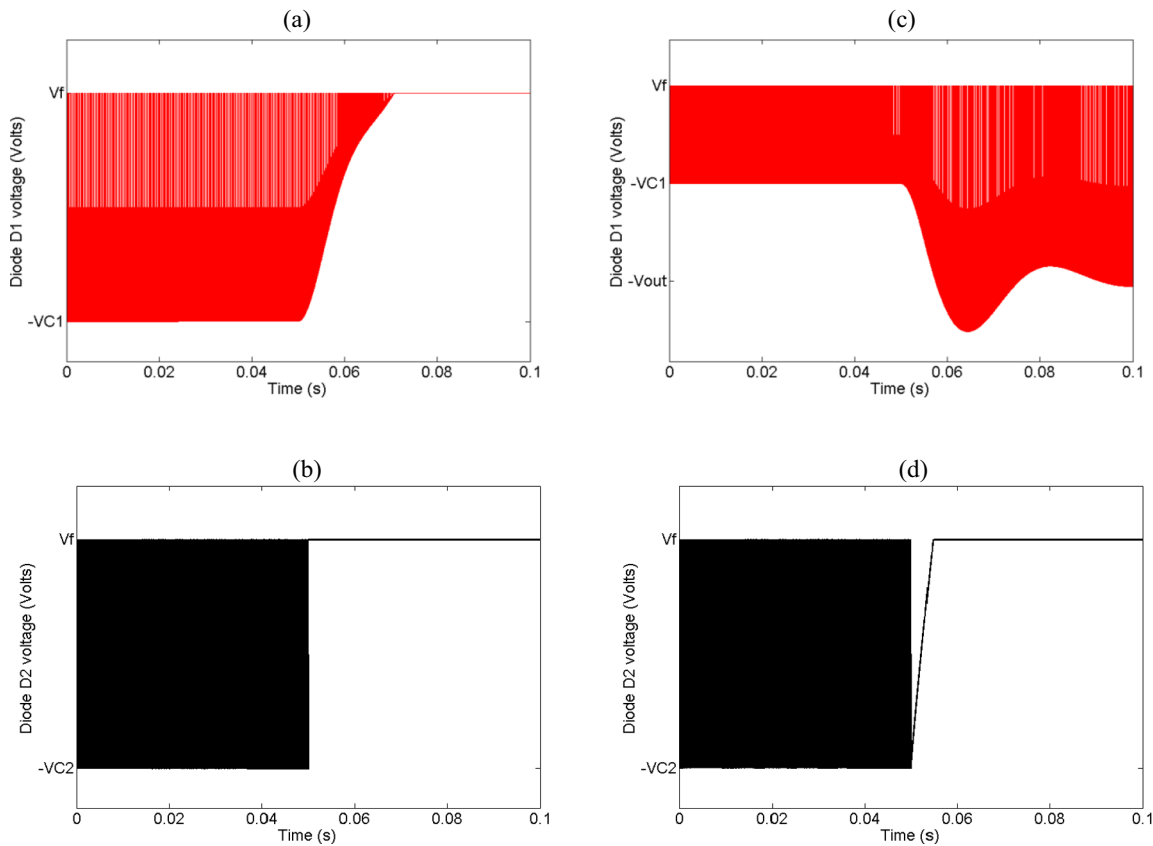


Fig. 4. Diodes voltages before and after SW2 fault occurrence at $t = 0.05$ s: (a) Diode D1 and (b) Diode D2 for open-circuit fault case; (c) Diode D1 and (d) Diode D2 for short-circuit fault case.

(SW2) is OFF. $VC1, VC2$, and V_f are capacitor C1 voltage, capacitor C2 voltage, and diode forward voltage drop, respectively.

During faulty operation, four cases could be distinguished: SW1 open-circuit, SW2 open-circuit, SW1 short-circuit and SW2 short-circuit. The possible converter electrical schemes related to these faulty modes are shown in Fig. 3.

3. Fault detection and reconfiguration method

In normal operation, diodes D1 and D2 are turning ON and OFF within a switching period. When a fault occurs in power switches SW1 or SW2, diodes D1 or D2 voltage is equal to V_f . For instance, diodes D1 and D2 voltages, before and after SW2 open and short circuit faults

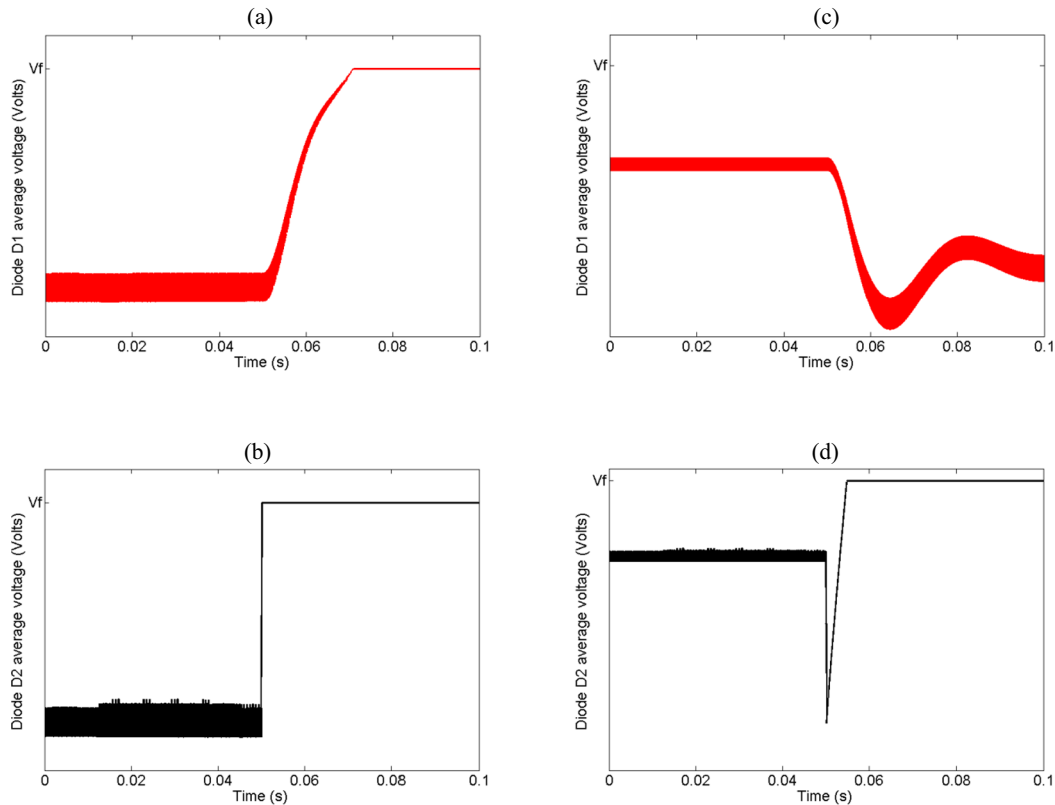


Fig. 5. Diodes average voltages before and after SW2 fault occurrence at $t = 0.05$ s: (a) Diode D1 and (b) Diode D2 average' voltages for open-circuit fault case; (c) Diode D1 and (d) Diode D2 average' voltages after for short-circuit fault case.

occurrence, are illustrated in Fig. 4. After SW2 open and short circuit fault occurrence, at $t = 0.05$ s, the nearby diode D2 becomes forward biased as indicated in Figs. 4(b) and (d). Therefore, diode D2 voltage is equal to V_f , while diode D1 voltage rises exponentially to V_f during SW2 open-circuit fault as shown in Fig. 4(a). Fig. 4(c) illustrates the case of SW2 short-circuit fault. The diode D1 maximum voltage changes from $-V_{C1}$ to $-V_{out}$ after fault occurrence, where V_{out} is the converter output voltage.

0–0 and 1–0 are the possible switches states after SW2 open circuit fault occurrence, as indicated in Table 1, where diode D2 is continuously forward biased. Since there is no state in which capacitor C1 could be charged (state 0–1), capacitors C1 is discharged in the load, which also make diode D1 continuously forward biased.

Since it is difficult to use diodes voltages to detect fault occurrence, the proposed fault detection method uses diodes D1 and D2 average voltages instead of real voltages. In fact, for the same faulty cases considered in Fig. 4, the diodes average voltages are illustrated in Fig. 5. When analyzing for example SW2 open circuit faulty case, one can see that diode D2 average voltage drops immediately to V_f after fault occurrence. Therefore, diodes average voltage is the parameter that allows detecting the fault presence and identifying the faulty switch.

During normal operation, the converter operates as a TLBDC by controlling SW1 and SW2, while SW3 remains uncontrolled. When diode D1 or D2 average voltage drops to V_f , it indicates that open circuit or short circuit fault occurrence either on switches SW1 or on SW2. After fault detection, the converter is reconfigured to operate as a two levels boost converter where SW3 switch is PWM controlled with a

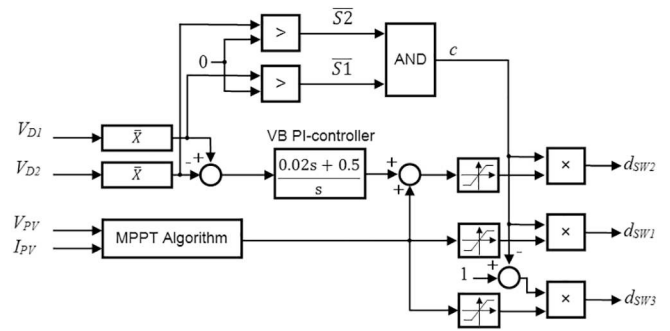


Fig. 6. TLBDC fault tolerant controller schema.

post-fault duty cycle. The switches SW1 and SW2 control signals become null.

4. Fault tolerant three-level boost DC-DC converter controller design

The implemented controller is shown in Fig. 6. Diodes D1 and D2 voltages, V_{D1} and V_{D2} , are sensed and their average values are then used to detect and locate the fault. Variable S2 and S1 indicates the faulty switch, if S1 (S2) is equal to 1 then the faulty switch is SW1 (SW2).

As shown in Fig. 7, Diodes D1 and D2 voltages are switching from V_f to $-V_{C1}$ and from V_f to $-V_{C2}$, respectively. This implies diodes

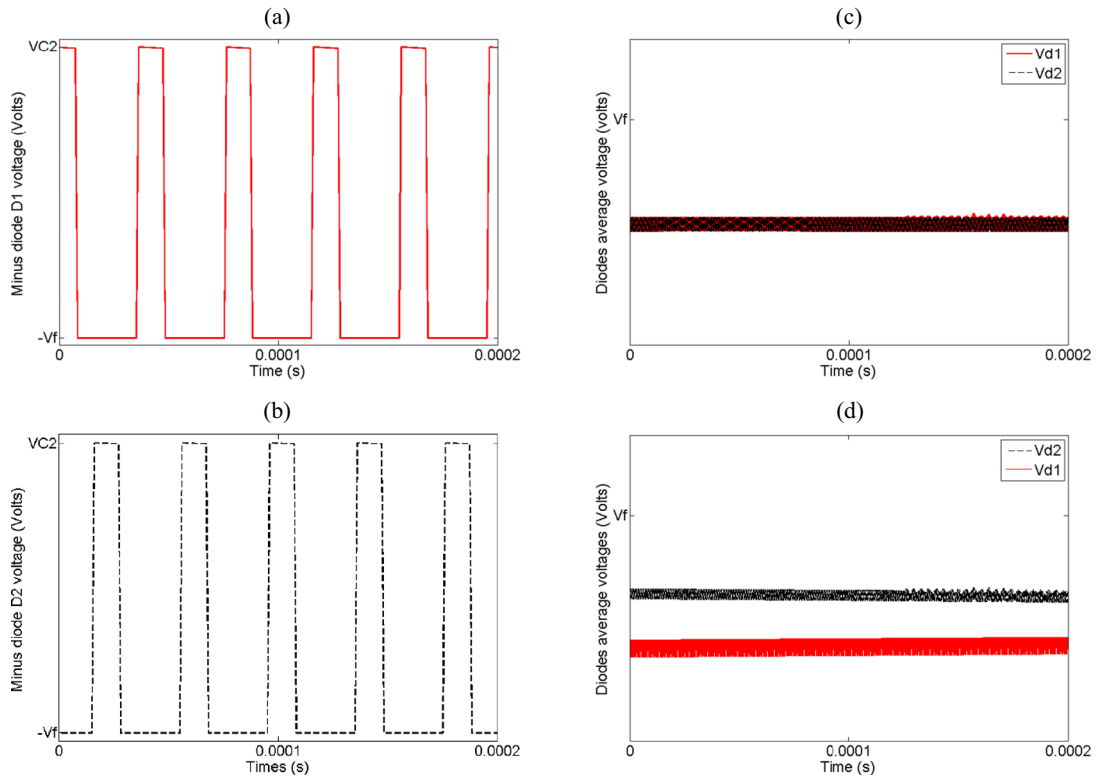


Fig. 7. Diodes voltages and average diodes voltages: (a) Minus diode D1 voltage, (b) minus diode D2 voltage, (c) diodes D1 and D2 average voltages for balanced capacitors voltages and (d) diodes D1 and D2 average voltages for unbalanced capacitors voltages.

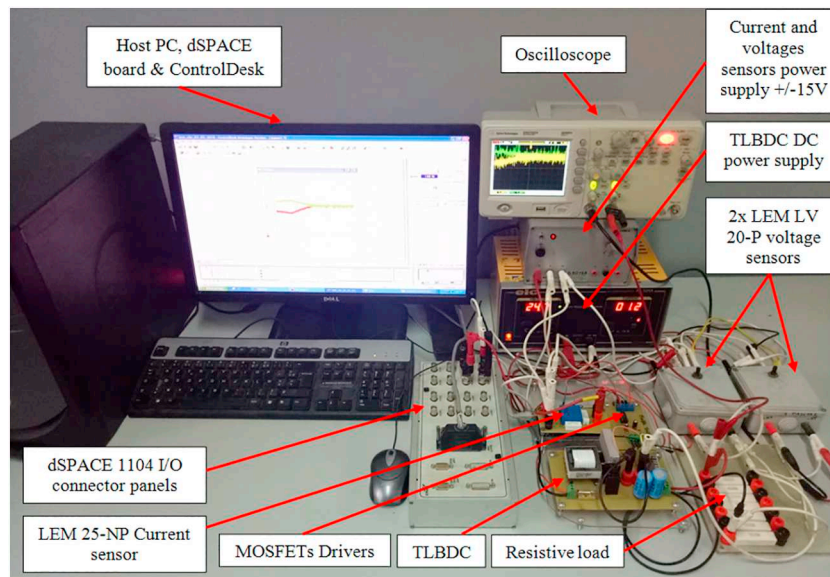


Fig. 8. Experimental setup.

switching from V_f to $V_C = -V_{C1} = -V_{C2}$ when capacitors voltages are equal. Which means that diodes average voltages are equal, as illustrated in Fig. 7 (c). In contrast, when capacitors voltages are unbalanced, diodes average voltages are not equal, as presented in Fig. 7

(d) (for $V_{C1} > V_{C2}$ case). Therefore, the difference between diodes average voltages is used as an input of a VB PI-controller whose parameters are indicated in Fig. 6. The VB controller aims to set the difference between those average voltages to zero. Using diodes average

Table 2
Converter parameters.

Parameter	Value
Switching frequency	12.5 KHz
Inductor	9 mH, internal resistance 0.1 Ω
Output capacitors	100 μ F, internal resistance 0.001 Ω
MOSFETs on resistance	0.1 Ω
Diode's forward voltage	0.5 V
Diode's internal resistance	0.001 Ω
Input voltage	25 V
Load	21 Ω

voltages for VB control allows avoiding the usage of extra voltage sensors for voltages VC1 and VC2 measurements.

Variables S1 and S2, indicated in Fig. 6, are equal to zero during normal operation and the parameter c is equal to 1. The PV voltage and current measurements are used by the MPPT algorithm for duty cycle calculation. The calculated duty cycle is used for SW1 switch PWM control signal generation, while the VB PI-controller output is added to this duty cycle and used to generate switch SW2 PWM control signal. Since switch SW3 control signal is multiplied by $1-c$. The latter is equal to zero in normal operation of TLBDC, which implies that SW3 control signal is equal to zero.

In faulty operation, either S1 or S2 is equal to 1 and the parameter c is null. The converter operates as a conventional two level DC-DC boost converter. The duty cycle generated by the MPPT algorithm is used for SW3 switch PWM control signal generation, while SW1 and SW2 switches control signals are equal to zero.

5. Results and discussions

In order to evaluate the effectiveness of the proposed strategy, simulation and experimental tests were carried out. Simulations were performed on Matlab/Simulink, while the experimental tests were performed using the experimental setup shown in Fig. 8. The converter parameters are listed in Table 2. For simplification purposes, a DC power supply was used as energy source instead of PV source.

The proposed fault tolerant strategy was experimentally implemented using the dSPACE 1104. The simplified scheme of experimental setup is shown in Fig. 9. After building the fault tolerant controller scheme based on real-time Simulink-blocks, including the dSPACE 1104 slave-PWM generator and A/D converters, the C code is automatically generated, downloaded and executed on the dSPACE board. The PWM signals phase-shifted by 180° were generated by the dSPACE 1104 and provided to IR2110 gates drivers that permits to control SW1, SW2 and SW3 switches. The ControlDesk monitor software was used to visualize and save the experimental data.

Figs. 10 and 11 show the simulation and experimental results of the proposed methodology, including the normal, the faulty, and the re-configuration states for an open and short circuit faults in power switch SW1.

Simulation results of two cases study are illustrated in Fig. 10. Figs. 10(a), (b) and (c) respectively show the capacitors voltages, output voltage and input power. In this case study, the VB control was applied at $t = 0.05$ s and an SW1 open circuit fault was occurred at $t = 0.1$ s. The short circuit case was also studied where the VB control was applied at $t = 0.05$ s and a SW1 short-circuit fault was occurred at $t = 0.1$ s. The capacitors voltages, output voltage and input power, are illustrated in Figs. 10(d), (e) and (f), respectively.

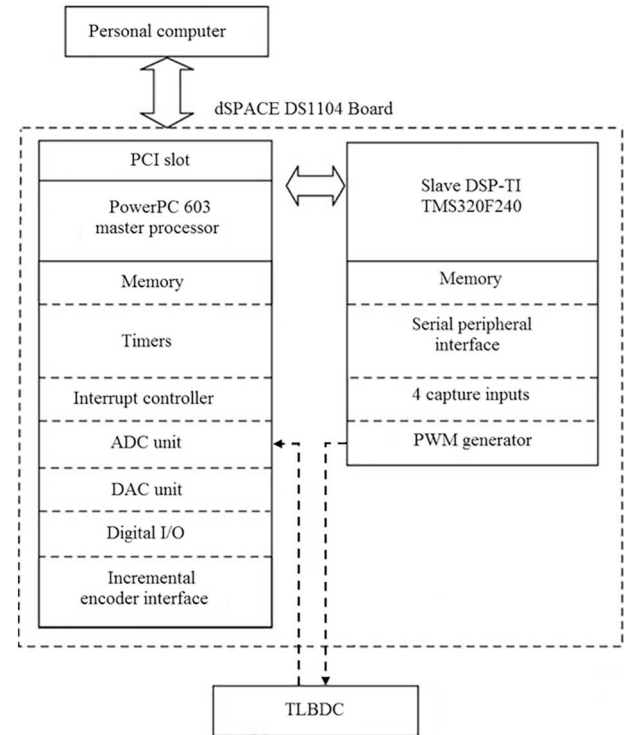


Fig. 9. Block-diagram of the dSPACE DS1104 controller board.

The fault cases that were studied on simulation were applied on the developed experimental setup. It was done to validate the simulation results. The experimental results of both fault cases are depicted in Fig. 11. The power switch open and short circuit faults were introduced by disabling the gate-drivers and turning on continuously the relevant faulty switch, respectively. Figs. 11(a), (b) and (c) respectively illustrate the measured capacitors voltages, output voltage and input power. In this case, VB control was applied at $t = 3.12$ s and SW1 open circuit fault was occurred at $t = 6.22$ s. For short circuit case, the VB control was applied at $t = 3.12$ s and SW1 short-circuit fault was occurred at $t = 6.24$ s, the capacitors voltages, output voltage and input power are illustrated in Figs. 11(d), (e) and (f), respectively.

By analyzing the obtained results, one can see that the experimental results are in good agreement with the simulation ones, except some differences in the response times. These differences are mainly due to delays included by D/A conversions, the processing time for real time implementation, and the calculation time of the voltages average values.

After applying the proposed VB control, the output capacitors voltages were balanced and the VB is kept as far as the fault is not detected. After the fault occurrence and detection, the converter is immediately reconfigured into a two-level boost converter with the same input power (50 watt) that was produced in the post fault. In addition, the converter output voltage is not changed. It is kept equals to 30 V before and after faults detection and reconfiguration.

The proposed fault-diagnosis method does not require extra sensors, since the number of sensors is the same as in conventional TLBDC control loop. However, for some faulty operation cases, higher stresses on the TLBDC switching components are induced due to the capacitors voltages unbalance. This is the only disadvantage of the proposed

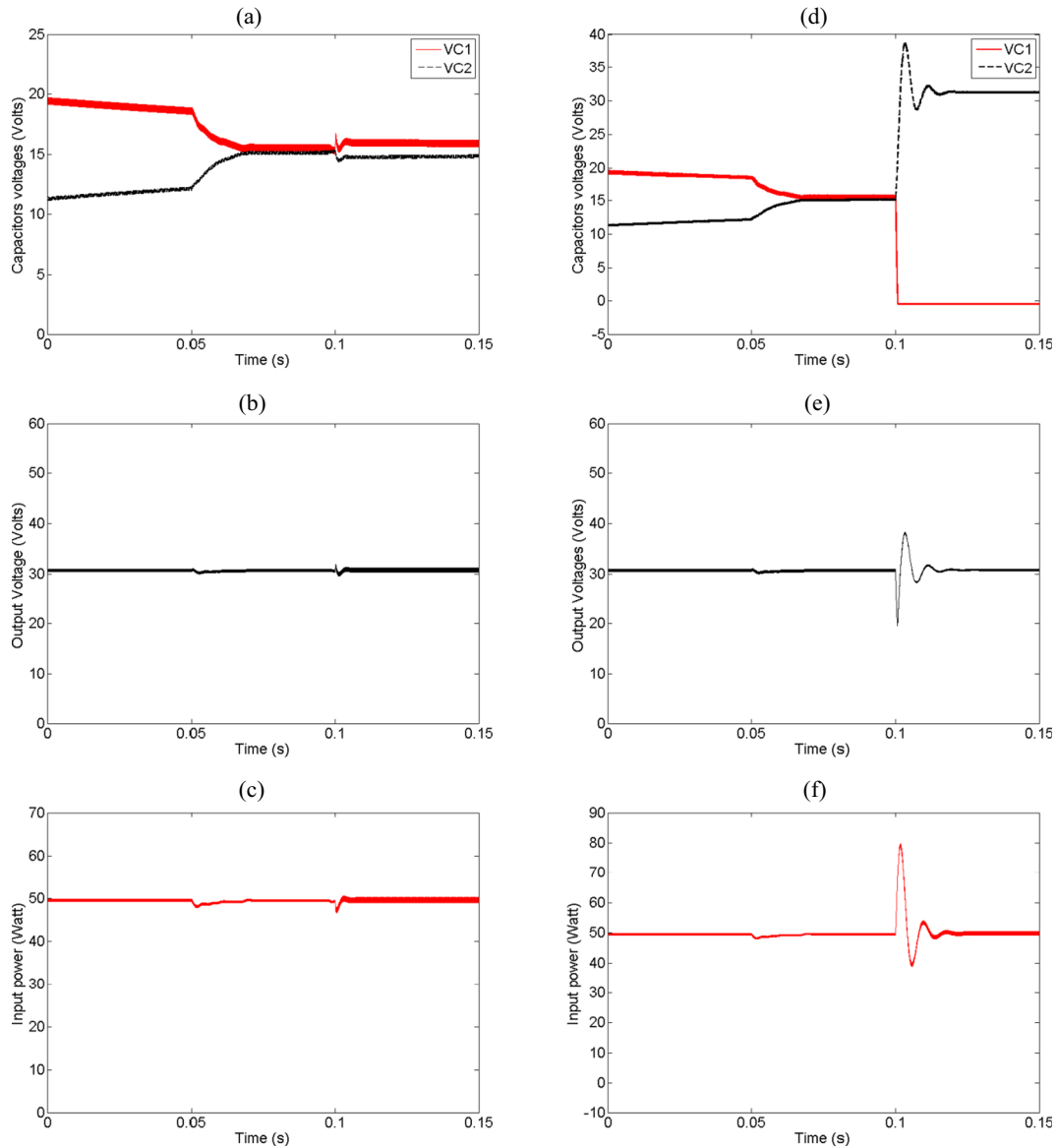


Fig. 10. Simulation results when VB control was applied at $t = 0.05$ s and SW1 fault occurrence at $t = 0.1$: (a) Capacitors voltages, (b) output voltage and (c) PV power for open circuit fault case; (d) Capacitors voltages, (e) output voltage and (e) input power for short circuit fault case.

strategy that should be taken into consideration during design process.

6. Conclusions

Switches open/short circuit faults diagnosis and a fault-tolerant TLBDC have been presented. The proposed fault tolerant method is effective, simple to implement, and does not require additional sensors, since it needs the same number of sensors used for conventional TLBDC control. It is based on diodes average voltages measurement for both fault detection and VB control. This method handles and locates any power switches open or short circuit faults and its implementation is effortless. One power switch is the only added device to the TLBDC scheme to perform fault tolerant operation.

The effectiveness of the proposed strategy was validated using simulation and experimental investigation. According to the obtained results, the fault-tolerant reconfiguration starts as soon as the faults occurred, and the converter topology is changed from a TLBDC to a two-level conventional boost converter.

The fault-tolerant operation of the converter results in higher stresses on the power components that should be taken into consideration in the design process, when choosing power switches and diodes. Even though, the reconfigured converter keeps providing the same power and output voltage as in the post fault. Moreover, the proposed fault tolerant TLBDC presents a low-cost choice rather than redundancy or multiphase topologies, and presents a better choice for PV and uninterrupted power supply applications.

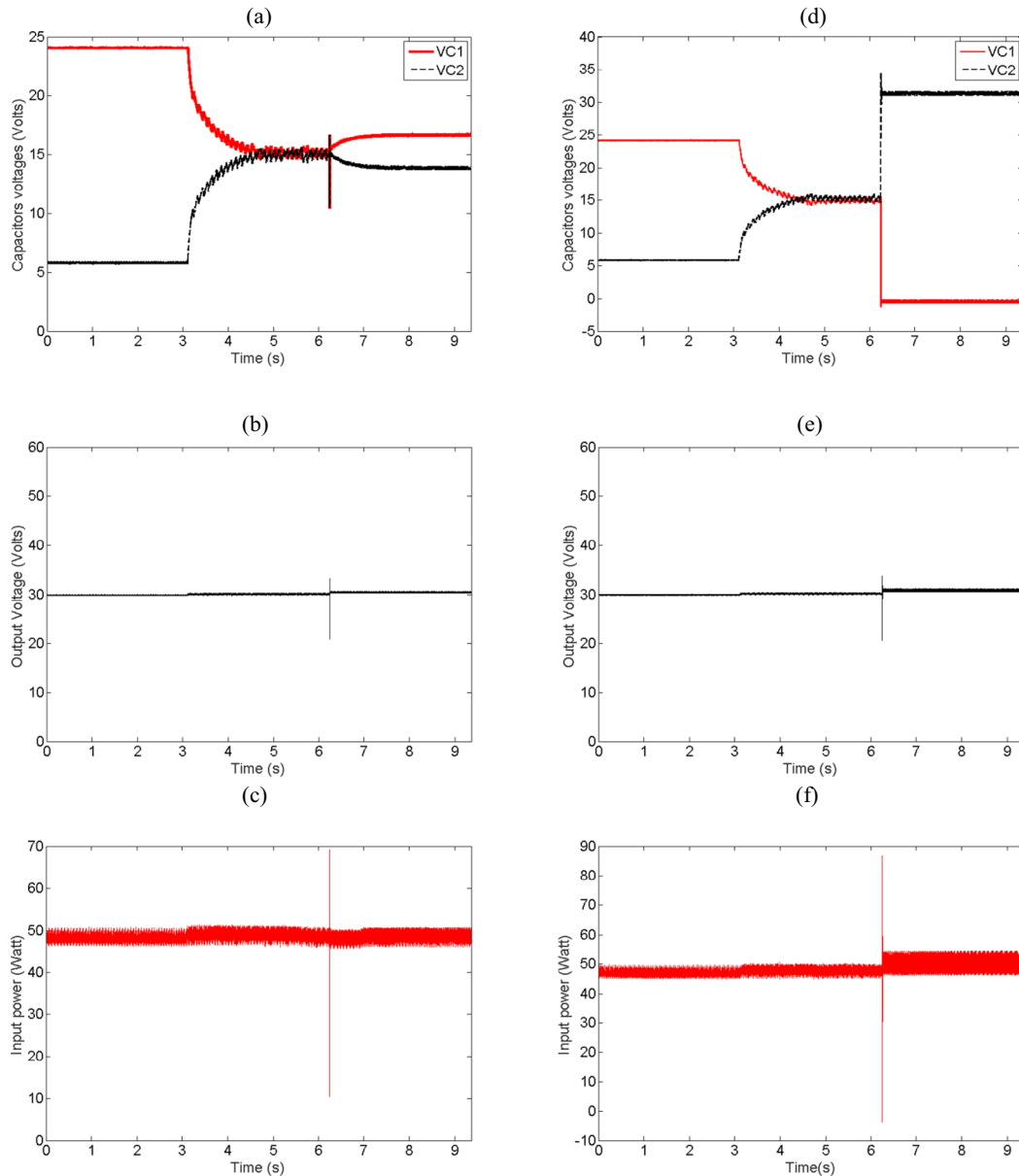


Fig. 11. Experimental results after applying VB control at $t = 3.12$ s and SW1 fault occurrence at $t = 6.22$: (a) Capacitors voltages, (b) output voltage and (c) PV power for open circuit fault case; (d) Capacitors voltages, (e) output voltage and (f) input power for short circuit fault case.

Acknowledgment

This work is performed in the framework of VERES Project funded by the Research Institute in Solar Energy and New Energies (IRESEN).

References

- [1] D. Oulad-abbou, S. Doubabi, A. Rachid, Solar charging station for electric vehicles, 3rd International Renewable and Sustainable Energy Conference (IRSEC), Marrakech, 2015, pp. 1–5.
- [2] D. Oulad-Abbou, S. Doubabi, A. Rachid, A power managing unit for mobile, stand-alone AC solar PV installations, 32nd European PV Solar Energy Conference and Exhibition (EU-PVSEC), Munich, 2016, pp. 2796–2800.
- [3] P. García-Triviño, J.P. Torreglosa, L.M. Fernández-Ramírez, F. Jurado, Control and operation of power sources in a medium-voltage direct-current microgrid for an electric vehicle fast charging station with a photovoltaic and a battery energy storage system, *Energy* 115 (2016) 38–48.
- [4] K.K. Tse, B.M.T. Ho, H.S.H. Chung, S.Y.R. Hui, A comparative study of maximum-power-point trackers for photovoltaic panels using switching-frequency modulation scheme, *IEEE Trans. Ind. Electron.* 51 (2004) 410–418.
- [5] Y.K. Lo, H.J. Chiu, T.P. Lee, I. Purnama, J.M. Wang, Analysis and Design of a Photovoltaic System DC connected to the utility with a power factor corrector, *IEEE Trans. Ind. Electron.* 56 (2009) 4354–4362.
- [6] H. Fakhham, D. Lu, B. Francois, Power control design of a battery charger in a hybrid active PV generator for load-following applications, *IEEE Trans. Ind. Electron.* 58 (2011) 85–94.
- [7] V. Salas, et al., Review of the maximum power point tracking algorithms for stand-alone photovoltaic systems, *Sol. Energy Mater. Sol. Cells* 90 (2006) 1555–1578.
- [8] W. Li, X. He, Review of nonisolated high-step-up DC/DC converters in photovoltaic grid-connected applications, *IEEE Trans. Ind. Electron.* 58 (2011) 1239–1250.
- [9] G. Dileep, S.N. Singh, Selection of non-isolated DC-DC converters for solar photovoltaic system, *Renew. Sust. Energy Rev.* 76 (2017) 1230–1247.
- [10] S.M. Reza Tousi, M.H. Moradi, N.S. Basir, M. Nemati, A function-based maximum power point tracking method for photovoltaic systems, *IEEE Trans. Power Electron.* 31 (2016) 2120–2128.
- [11] E. Ribeiro, A.J.M. Cardoso, C. Boccaletti, Fault-tolerant strategy for a photovoltaic DC-DC converter, *IEEE Trans. Power Electron.* 28 (2013) 3008–3018.
- [12] J. Li, A.Q. Huang, Z. Liang, S. Bhattacharya, Analysis and design of active NPC (ANPC) inverters for fault-tolerant operation of high-power electrical drives, *IEEE Trans. Power Electron.* 27 (2) (Feb. 2012) 519–533.
- [13] J. Estima, A.J.M. Cardoso, A new algorithm for real-time multiple open-circuit fault diagnosis in voltage-fed PWM motor drives by the reference current errors, *IEEE Trans. Ind. Electron.* 60 (2012) 3496–3505.
- [14] F. Ben Youssef, L. Sbita, Sensors fault diagnosis and fault tolerant control for grid connected PV system, *Int. J. Hydrog. Energy* vol. 42, (13) (2017) 8962–8971.
- [15] T. Wang, J. Qi, H. Xu, Y. Wang, L. Liu, D. Gao, Fault diagnosis method based on

- FFT-RPCA-SVM for cascaded-multilevel inverter, *ISA Trans.* 60 (2016) 156–163.
- [16] Z. Wang, Y. Wang, J. Chen, M. Cheng, Fault-tolerant control of NPC three-level inverters-fed double-stator-winding PMSM drives based on vector space decomposition, *IEEE Trans. Ind. Electron.* 64 (2017) 8446–8458.
- [17] S. Xu, J. Zhang, J. Hang, Investigation of a fault-tolerant three-level T-type inverter system, *IEEE Trans. Ind. Appl.* 53 (2017) 4613–4623.
- [18] X. Pei, S. Nie, Y. Chen, Y. Kang, Open-circuit fault diagnosis and fault-tolerant strategies for full-bridge DC–DC converters, *IEEE Transactions on Power Electronics*, vol. 27, 2012, pp. 2550–2565.
- [19] H. Qingchuan, C. Wenhua, P. Jun, Q. Ping, A prognostic method for predicting failure of dc/dc converter, *Microelectron. Reliab.* 74 (2017) 27–33.
- [20] R. Jayabalan, B. Fahimi, Monitoring and fault diagnosis of DC-DC multistage converter for hybrid electric vehicles, 2005 5th IEEE International Symposium on Diagnostics for Electric Machines, Power Electronics and Drives, vols. 1–6, Vienna, Austria, 2005.
- [21] S.Y. Kim, K. Nam, H.S. Song, H.G. Kim, Fault diagnosis of a ZVS DC–DC converter based on DC-link current pulse shapes, *IEEE Trans. Ind. Electron.* 55 (2008) 1491–1494.
- [22] H. Li, Z. Guo, C. Liu, T.Q. Zheng, An extensible stability analysis method in time domain for cascaded DC-DC converters in electrical vehicles, *Microelectron. Reliab.* (2018) 88–90.
- [23] Y. Chen, X. Pei, S. Nie, Y. Kang, Monitoring and diagnosis for the DC–DC converter using the magnetic near field waveform, *IEEE Trans. Ind. Electron.* 58 (2011) 1634–1647.
- [24] A. Nouri, I. Salhi, S. El Beid, N. Essounbouli, E. Elwarraki, A fault tolerant strategy for multilevel dc-dc converters to improve the PV system efficiency, *IFAC-PapersOnLine* 49 (2016) 704–709.
- [25] Ghazanfari, Y.A.R.I. Mohamed, A resilient framework for fault-tolerant operation of modular multilevel converters, *IEEE Trans. Ind. Electron.* vol. 63, (5) (May 2016) 2669–2678.
- [26] Y. Lian, D. Holliday, S. Finney, "Modular input-parallel output-series DC/DC converter control with fault detection and redundancy," in *IET generation, Transm. Distrib.* 10 (2016) 1361–1369.
- [27] K.A. Ambusaidi, V. Pickert, B. Zahawi, Computer aided analysis of fault tolerant multilevel DC/DC converters, 2006 International Conference on Power Electronic, Drives and Energy Systems, 1–6 2006 (New Delhi, India).
- [28] S. Dusmez, M. Bhardwaj, L. Sun, B. Akin, A software frequency response analysis method to monitor degradation of power MOSFETs in basic single-switch converters, 2016 IEEE Applied Power Electronics Conference and Exposition (APEC), Long Beach, CA, 2016, pp. 505–510.
- [29] S. Gowtham, M. Balaji, S. Harish, M.S. Abraham Pinto, G. Jagadeesh, Fault tolerant single switch PWM DC-DC converters for battery charging applications, *Energy Procedia* 117 (2017) 753–760.
- [30] X. Pei, S. Nie, Y. Chen, Y. Kang, Open-circuit fault diagnosis and fault-tolerant strategies for full-bridge DC–DC converters, *IEEE Transactions on Power Electronics*, Vol. 27 2012, pp. 2550–2565.
- [31] D. Oulad-Abbou, S. Doubabi, A. Rachid, Voltage balance control analysis of three-level boost DC-DC converters: theoretical analysis and DSP-based real time implementation, *Energies* 11 (11) (2018) 3073.